Influences of benthic infaunal burrows on community structure and activity of ammonia-oxidizing bacteria in intertidal sediments

Running title: Community structure and activity of AOB in infaunal burrows

By

Hisashi Satoh, Yoshiyuki Nakamura, Satoshi Okabe*

Department of Urban and Environmental Engineering, Graduate School of Engineering, Hokkaido University, North-13, West-8, Sapporo 060-8628, Japan.

* *Corresponding Author*

Satoshi OKABE

Department of Urban and Environmental Engineering, Graduate School of Engineering, Hokkaido University, North-13, West-8, Sapporo 060-8628, Japan.

Tel.: +81-(0)11-706-6266

Fax.: +81-(0)11-706-6266

E-mail: sokabe@eng.hokudai.ac.jp

ABSTRACT

Influences of benthic infaunal burrows constructed by the polychaete (*Tylorrhynchus heterochaetus*) on O_2 concentrations and community structures and abundances of ammonia-oxidizing bacteria (AOB) and nitrite-oxidizing bacteria (NOB) in intertidal sediments were analyzed by the combined use of a 16S rRNA gene-based molecular approach and microelectrodes. The microelectrode measurements performed in an experimental system developed in an aquarium showed direct evidence of O_2 transport down to a depth of 350 mm of the sediment through a burrow. The 16S rRNA gene-cloning analysis revealed that the betaproteobacterial AOB communities in the sediment surface and the burrow walls were dominated by *Nitrosomonas* sp. Nm143-like sequences and most of the clones in *Nitrospira*-like NOB clone libraries of the sediment surface and the burrow walls were related to the *Nitrospira marina* lineage. Furthermore, we investigated vertical distributions of AOB and NOB in the infaunal burrow walls and the bulk sediments by real-time quantitative polymerase chain reaction (Q-PCR) assay. The AOB and *Nitrospira*-like NOB specific 16S rRNA gene copy numbers in the burrow walls were comparable with those in the sediment surfaces. These numbers in the burrow wall at a depth of 50-55 mm from the surface were, however, higher than those in the bulk sediment at the same depth. The microelectrode measurements showed higher NH_4^+ consumption activity at the burrow wall as compared with those at the surrounding sediment. This result was consistent with the results of microcosm experiments showing that the consumption rates of NH_4^+ and total inorganic nitrogen increased with increasing infaunal density in the sediment. These results clearly demonstrated that the infaunal burrows stimulated O_2 transport into the sediment in which otherwise reducing conditions prevailed, resulting in

development of high NH_4^+ consumption capacity. Consequently, the infaunal burrow became an important site for NH_4^+ consumption in the intertidal sediment.

INTRODUCTION

Benthic infaunal activities, such as burrow formation, burrow irrigation, defecation, and excretion of soluble and insoluble metabolites, increase the surface area across which solutes can diffuse into or out of the sediments and the substrate availability for inhabiting microorganisms (5, 13, 17, 24, 25, 32, 34). These burrows also provide a more stable physical environment compared to bulk sediment. Therefore, the sediment surrounding the infaunal burrows (i.e., burrow walls) could have markedly higher levels of microbial biomass, diversity, and activity compared with the bulk sediment. Previous studies have revealed that benthic infaunal activities resulted in changes in biogeochemical characteristics and microbial community structures in sediments (20, 22, 31). Although many studies demonstrated that presence of benthic infauna strongly affects the microbial ecology of estuarine sediments, surprisingly little attention has been paid to bioturbation effects on nitrification. In estuarine systems with high inputs of nitrogenous compounds, sediment is a major site for nitrification due to abundance of ammonia-oxidizing bacteria and their high activities (1). One such estuarine is the Niida River estuary in Hachinohe city, Japan, where the water quality deterioration (e.g. presence of organic carbon and NH_4^+) is evident, mainly due to the discharge of treated and untreated domestic and industrial wastewater and urban and agricultural run-off (26, 27).

The solute concentrations in an infaunal burrow have been measured by collecting the liquid samples in a burrow (17). This method was not completely satisfying because the

concentration measured was the mean value throughout the burrow. Application of microelectrodes has enabled direct measurements of O_2 and nutrients in burrows without sampling. Applications of O_2 microelectrodes revealed presence of O_2 in infaunal burrows (5), in the burrows of freshwater insects (34), and in an actively ventilated polychaete burrow (13). NH_4^+ concentration profiles in freshwater sediments as influenced by insect larvae were also measured by NH_4^+ microelectrodes (1). These studies have demonstrated evidence of enhanced mass transport through the burrows. However, the measurements were limited in just a few cm depths from the sediment surface due to low accessibility of the microelectrodes and the uncertainty of exact position of the burrow.

Microbial community structures in infaunal burrows and tubes have been investigated by 16S rRNA gene-cloning analysis (20, 22) and ester-linked phospholipid fatty acid analysis (31). These studies have provided a good understanding of the microbial community structure and diversity in the burrow and sediment, and allowed comparison with biogeochemical characteristics. One study revealed that the microbial community structures in burrow walls were different from those in the bulk sediment (31). However, community structure, abundance and *in situ* activity of nitrifying bacteria in infaunal burrows and bulk sediment have not been analyzed, compared, and linked to available O_2 concentrations in the burrows.

Therefore, we have investigated the influences of infaunal burrows on microbial community structures and the abundance of ammonia-oxidizing bacteria (AOB) and nitrite-oxidizing bacteria (NOB) and *in situ* activities of AOB in intertidal sediments by applying 16S rRNA gene-cloning analysis, real-time quantitative polymerase chain reaction (Q-PCR) assay and microelectrodes. The Niida River estuarine sediment was selected, in

which a high number of infaunal burrows were constructed by the benthic infaunas, *Tylorrhynchus heterochaetus*, which generally inhabited in the intertidal zone of the Japanese estuary. To directly measure *in situ* O_2 concentration profiles in the burrows, we have constructed a continuous flow aquarium with agar slits in a sideboard, through which microelectrodes could be inserted into the burrow.

MATERIALS AND METHODS

Sampling

River water and sediment samples were collected as described below during the low tide at an intertidal area of the Niida River, Hachinohe city, Japan, which was located approximately 1.5 km from the river mouth (27). The samples were immediately transferred to the laboratory and were analyzed within 12 h.

Microcosm experiments

Microcosm experiments were carried out to determine the influence of infaunal density on the consumption rates of NH_4^+ and total inorganic nitrogen (N_i) that was defined as the sum of the concentrations of NH_4^+, NO_2^- and NO_3^-. Grab samples of sediments were obtained at the study site and passed through a 1-mm mesh to remove pebbles, large detritus particles and indigenous infaunas. After thorough mixing the sediments were apportioned into cylindrical sediment containers (11.4 cm in diameter and 30 cm height) to give a final sediment height of 30 cm. Various numbers of *T. heterochaetus* were placed on the sediment surface in each microcosm and allowed to burrow into the sediments. They generally burrowed within a few minutes. The sediment surfaces in the microcosms were covered

with 1-mm meshes to prevent the infaunas from moving out of the microcosms. Then, the microcosms were buried in the sediment at the study site, where the surfaces of the microcosms were aligned with the surface of the natural sediment at the study site. The microcosms were allowed to stabilize for 2 to 3 weeks. Then each microcosm was brought to the laboratory and placed in an aquarium filled with 3 liters of the river water collected at the same site. NH_4Cl and $NaNO_3$ were added to the river water, resulting in final concentrations of approximately 360 μM of NH_4^+ and NO_3^-, respectively. O_2 concentration of the overlaying water was kept ca. 210 μM by continuously bubbling with air. The microcosms were incubated for 48 h in the dark. The changes in NH_4^+, NO_2^- and NO_3^- concentrations in the overlying water were monitored with time. The consumption rates of NH_4^+ ($R(NH_4^+)$) and N_i ($R(N_i)$) were calculated from the decreases in NH_4^+ and N_i concentrations during the initial 12-h incubation, respectively. In total, 16 microcosm experiments were conducted with different infaunal densities.

Microelectrode measurements

The concentration profiles of O_2 and NH_4^+ in the sediment were measured in the laboratory using microelectrodes as described by Nakamura et al. (26). Clark-type microelectrodes for O_2 were prepared and calibrated as described by Revsbech (30). The LIX-type microelectrodes for NH_4^+ were constructed, calibrated, and used according to the protocol described by de Beer et al. (9) and Okabe et al. (28). To directly monitor O_2 concentrations inside an infaunal burrow along the depth, we constructed an aquarium with an acrylic plate (20 cm wide, 1 cm thick and 50 cm height) (see **Fig. S1** in the supplemental material). There were 45 slits (0.5 × 5 cm), which were filled with 3% agar plate, in one side

of the aquarium (see **Fig. S1C** in the supplemental material). By this means, we could determine the burrow structure and microelectrode position in the burrow. The aquarium was filled with the sediment collected in the same way as that for the microcosm experiments. An infauna (*T. heterochaetus*) was placed on the sediment surface and allowed to burrow. River water was continuously fed to the aquarium at a flow rate of 2 ml min^{-1}. The aquarium was maintained at 20°C in the dark. After 3 days, the infauna created a visible burrow. For the measurements of O_2 concentrations inside the infaunal burrow, the O_2 microelectrode was inserted into the burrow through the agar plate.

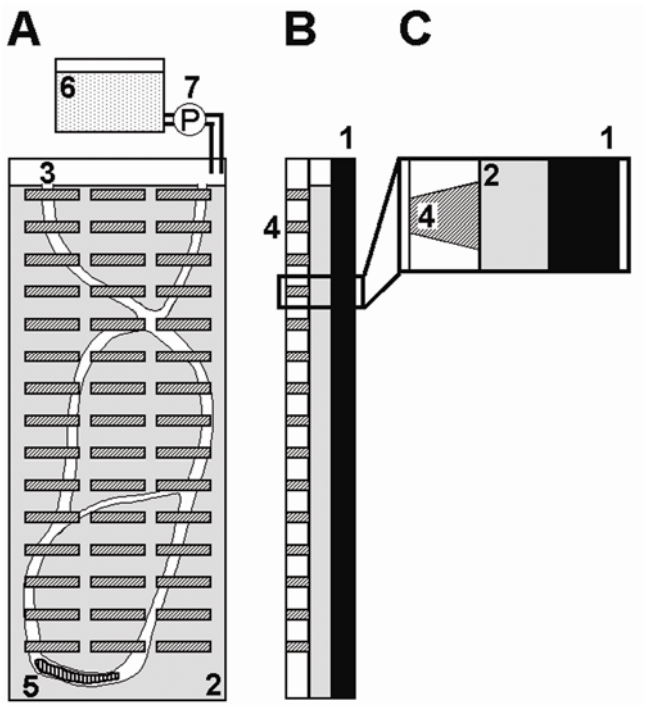

Fig. S1. Experimental apparatus for monitoring O_2 concentrations in an infaunal burrow: 1, sideboard; 2, sediment; 3, an infaunal burrow; 4, agar plates; 5, an infauna; 6, a tank filled with river water; 7, a pump. (A) A front view. (B) A side view. (C) A close-up view of the side view enclosed by the box in panel B.

In order to analyze NH_4^+ consumption rates in the burrow wall, the concentration profiles of O_2 and NH_4^+ were measured at a cross-section of the sediment in the aquarium. A synthetic medium was used to avoid interference with the LIX-type microelectrodes for NH_4^+ (26). The sediment was incubated in the medium at 20°C for more than 30 min before measurements to ensure that steady-state profiles were obtained. Three concentration profiles were measured for each chemical species and at each measuring point. The details of microelectrode measurements are described elsewhere (26, 27). Based on the O_2 and NH_4^+ concentration profiles measured, the total O_2 and NH_4^+ consumption rates were calculated using Fick's first law of diffusion (26, 27). The molecular diffusion coefficients used for the calculations were 2.09×10^{-5} cm^2 s^{-1} for O_2 in liquid, 1.38×10^{-5} cm^2 s^{-1} for NH_4^+ in liquid (3), and 2.2×10^{-5} cm^2 s^{-1} for O_2 in 3% agar plate at 20°C (16). Differences between the rates were statistically analyzed by *t* test.

DNA extraction and PCR amplification

Three sediment samples (approximately 1 cm^3) were collected with sterile spatulas at different points corresponding to each sampling position (i.e., sediment surface, bulk sediment, and burrow walls at depths of 25-30 mm and 50-55 mm). DNA was extracted from each sample (approximately 0.2 cm^3) using a Fast DNA spin kit (Bio 101, Qbiogene Inc., Carlsbad, Calif) as described in the manufacturer's instructions. The 16S rRNA gene fragments from the extracted total DNA were amplified with EX Taq DNA polymerase (TaKaRa Bio Inc., Ohtsu, Japan) by using the AOB specific primer set CTO189fA/B, CTO189fC and CTO654r (18) as well as the *Nitrospira*-like NOB specific primer set of Ntspa685 (15) and NTSPAf (26). The PCR conditions used for AOB and *Nitrospira*-like

NOB were described by Hermansson and Lindgren (14) and Nakamura et al. (26). PCR products were electrophoresed on a 1% (wt/vol) agarose gel. To reduce the possible bias caused by PCR amplification, the 16S rRNA gene was amplified in triplicate tubes for each sample, and then in total 9 PCR products were combined for the next cloning step.

Cloning and sequencing of the 16S rRNA gene and phylogenetic analysis

The purified PCR products were ligated into a pCR-XL-TOPO® vector and transformed into ONE SHOT *Escherichia coli* cells following the manufacturer's instructions (TOPO® XL PCR cloning; Invitrogen). Partial sequencing of 16S rRNA gene inserts (465 bp for AOB and 510 bp for *Nitrospira*-like NOB) was performed using an automatic sequencer (ABI Prism 3100 Avant Genetic Analyzer; Applied Biosystems) with a BigDye terminator Ready Reaction kit (Applied Biosystems). All sequences were checked for chimeric artifacts by the CHECK_CHIMERA program in the Ribosomal Database Project (21) and compared with similar sequences of the reference organisms by a BLAST search (2). Sequence data were aligned with the CLUSTAL W package (33). Clones with more than 97% sequence similarity were grouped into the same operational taxonomic unit (OTU), and their representative sequences were used for phylogenetic analysis.

Quantification of AOB and Nitrospira- and Nitrobacter-like NOB by Q-PCR.

Sediment samples were collected from sediment surface, burrow walls and bulk sediments at depths of 5-10 mm, 25-30 mm and 50-55 mm as described above. Total cell counts were performed after the diluted sediment samples on 0.2-μm-membrane filters were stained with 6-diamidino-2-phenylindole (DAPI). At least 15 replicate analyses were

performed for each sample. Q-PCR assays were performed to quantify AOB and *Nitrospira*- and *Nitrobacter*-like NOB specific 16S rRNA genes. The Q-PCR assay for betaproteobacterial AOB and *Nitrospira*-like NOB was performed as described previously (14, 26). The Q-PCR assay for *Nitrobacter*-like NOB was performed in total volume of 25 µl with 12.5 µl of SYBR Green PCR Master Mix (Applied Biosystems), 7.5 pmol of each of the forward and reverse primers (FGPS872f and FGPS1269r) (10), 2.5µl of bovine serum albumin solution (Invitrogen) and either 0.1 pg of sample DNA or 10 to 10^5 copies per well of the standard bacterium DNA of *Nitrobacter winogradskyi* (NBRC 14297). All Q-PCRs were performed in MicroAmp Optical 96-well reaction plates with optical cap (PE Applied Biosystems). The template DNA in the reaction mixtures was amplified and monitored with an ABI prism 7000 Sequence Detection System (PE Applied Biosystems). The cycling regime for AOB and *Nitrospira*-like NOB was as follows: hold for 2 min at 50°C; hold for 10 min at 95°C; and 40 cycles of 15 sec at 95°C and 1 min at 60°C. The cycling regime for *Nitrobacter*-like NOB was as follows: hold for 2 min at 50°C; hold for 10 min at 95°C; and 80 cycles of 15 sec at 95°C and 1 min at 50°C. The detection limits for AOB, *Nitrospira*- and *Nitrobacter*-like NOB in this study were 2.7×10, 1.6×10^2 and 5.4×10 copies per well, respectively, which correspond to 6.7×10^4, 4.0×10^4 and 1.4×10^4 copies cm^{-3} when the sediment sample volume and DNA extraction step are taken into account. Four replicate analyses were performed for each sample. A *t* test was applied to evaluate differences of the total bacterial cells and AOB and *Nitrospira*-like NOB specific 16S rRNA gene copy numbers among the samples.

Analytical methods

The NH_4^+ concentrations were colorimetrically determined (6) and the NO_2^- and NO_3^- concentrations were determined using an ion chromatograph (HIC-6A; Shimadzu) equipped with a Shim-pack IC-AI column. The samples for NH_4^+, NO_2^- and NO_3^- were filtered through 0.2-μm-membrane filters before the analysis. The O_2 concentration and pH in the overlaying water were directly determined using an O_2 and a pH electrode, respectively.

Nucleotide sequence accession numbers

The GenBank/EMBL/DDBJ accession numbers for the 16S rRNA gene sequences of representative 35 clones used for the phylogenetic analysis are AB239541, AB239545, AB239546, AB239560, AB239561, AB239566, and AB264558 to AB264586.

RESULTS AND DISCUSSION

Sediment characteristics

Many burrow openings with approximately 5 mm in diameter were found on the sediment surface at the study site during the low tide. Three types of benthic infaunas inhabited in the sediment. Numerically most abundant species was *T. heterochaetus* (84%) whereas the densities of *Notomastus* sp. (11%) and *Neanthes japonica* (5%) were low. Because the size of *T. heterochaetus* was much bigger (approximately 5 mm in diameter) than other two species (<1 mm in diameter), we speculated that all of the visible burrows were created by *T. heterochaetus*. The visible burrows extended down to a depth of at least 350 mm. Density of benthic infaunas in the upper 350 mm of the sediment was ca. 5700 individuals m^{-3}. Assuming a burrow of *T. heterochaetus* to be a straight tube with 5 mm in

diameter and 350 mm in length, the specific surface area of the burrow walls in the upper 350 mm of the sediment was calculated to be 26.4 m^2 m^{-3}. The burrow walls were covered with thin oxidized-light brown layers. The color of the burrow wall was similar to that of the sediment surface. Average NH_4^+, NO_2^- and NO_3^- concentrations (± standard deviation) in the overlaying water were 44±39 μM, 1±5 μM and 127±168 μM, respectively (n = 57). During the high tide, we occasionally found that suspended particles flew into the burrow and the fluffy biofilm developed at the burrow opening oscillated, indicating the overlaying water was introduced into the burrow. In contrast, the water in burrows stood during the low tide. Thus, we expected that the local environment in the burrows (i.e., the concentrations of O_2, NH_4^+, NO_2^- and NO_3^-) was dynamically changing with time as compared with that in the river water. Further information on the sediment at the study site and the physical and chemical parameters in river water can be found elsewhere (26, 27).

Microcosm experiments

The consumption rates of NH_4^+ ($R(NH_4^+)$) and N_i ($R(N_i)$) of the sediments with various benthic infaunal densities (i.e., *T. heterochaetus*) were determined in the microcosm experiments (**Fig. 1**). Mean values (± standard deviation) of $R(NH_4^+)$ and $R(N_i)$ of the sediment without the infauna were 670 ± 540 μmol m^{-2} h^{-1} and 1260 ± 770 μmol m^{-2} h^{-1}, respectively. Both rates increased as infaunal density increased. The increase in the $R(N_i)$ was more significant as compared with the $R(NH_4^+)$.

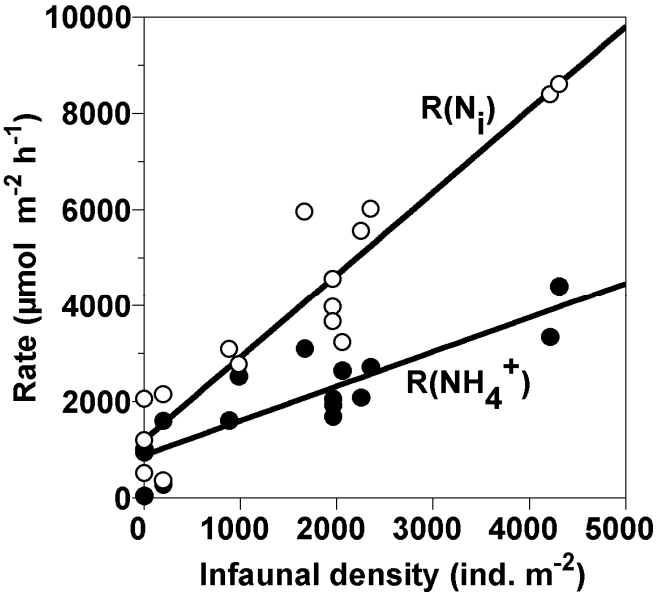

Fig. 1. The consumption rates of NH_4^+ ($R(NH_4^+)$) and total inorganic nitrogen ($R(N_i)$) of the sediment as a function of the density of *T. heterochaetus* in the microcosm experiments. The solid lines indicate linear regression of the data. The equations of the straight lines were $y = 0.72x + 890$ with $r^2 = 0.75$ (NH_4^+ consumption) and $y = 1.72x + 1200$ with $r^2 = 0.88$ (total inorganic nitrogen consumption).

Community structures of AOB and NOB

Three 16S rRNA gene clone libraries of AOB belonging to the *Betaproteobacteria* were constructed from three sediment samples taken from the sediment surface (SS) and the burrow walls at depths of 25-30 mm (BW-25) and 50-55 mm (BW-50) (**Table 1** and **Fig. S2** in the supplemental material). Sixty-seven, forty-seven and fifty-two clones were randomly selected from the SS, BW-25 and BW-50 clone libraries, respectively, and the partial sequences of 465 bp were analyzed. In total, the clones were grouped into 27 OTUs, and their representative sequences were used for phylogenetic analysis (**Fig. S2**). According to Purkhold et al. (29), we classified the *betaproteobacterial* AOB into seven stable lineages

(*Nitrosomonas oligotropha*, *Nitrosomonas marina*, *Nitrosomonas cryotoleransa*, *Nitrosomonas europaea*/*Nitrosococcus mobilis*, *Nitrosomonas communis*, *Nitrosomonas* sp. Nm143, and *Nitrosospira briensis*). In all three samples the most frequently detected clones were affiliated with the *Nitrosomonas* sp. Nm143 lineage with 93-99% sequence similarity (**Table 1**). These clones represented 30, 62 and 44% of the total clones recovered from the SS, BW-25 and BW-50 samples, respectively. *Nitrosomonas* sp. Nm143-like sequences have been found at intermediate salinity sites of other estuaries (4, 12). The second frequently detected clones recovered from the SS and BW-25 samples were affiliated with the *Nitrosomonas marina* lineage (the detection frequency of 9 and 19%, respectively), whereas the second frequently detected clones were affiliated with the *Nitrosospira briensis* lineage (the detection frequency of 17%) in the BW-50 samples. *Nitrosomonas marina*-like sequences have also been detected in relatively high-salinity environments (7, 12), because the *N. marina* lineage comprises obligate halophilic and salt-tolerant species. Thus, the AOB community structures in the burrow walls were similar to that in the sediment surface. This reflected the transport of overlying water into the burrows as confirmed by the microelectrode measurements. In this study, we focused only on the community structure of aerobic AOB affiliated with the *betaproteobacteria* whereas other ammonia-oxidizing microorganisms (e.g, anaerobic ammonium-oxidizing bacteria (i.e., ANAMMOX bacteria), the genus *Nitrosococcus* affiliated with the *gammaproteobacteria* and ammonia-oxidizing *Crenarchaea*) have not been analyzed. Contribution of these AOB to NH_4^+ oxidation in the sediment should be examined in the future study.

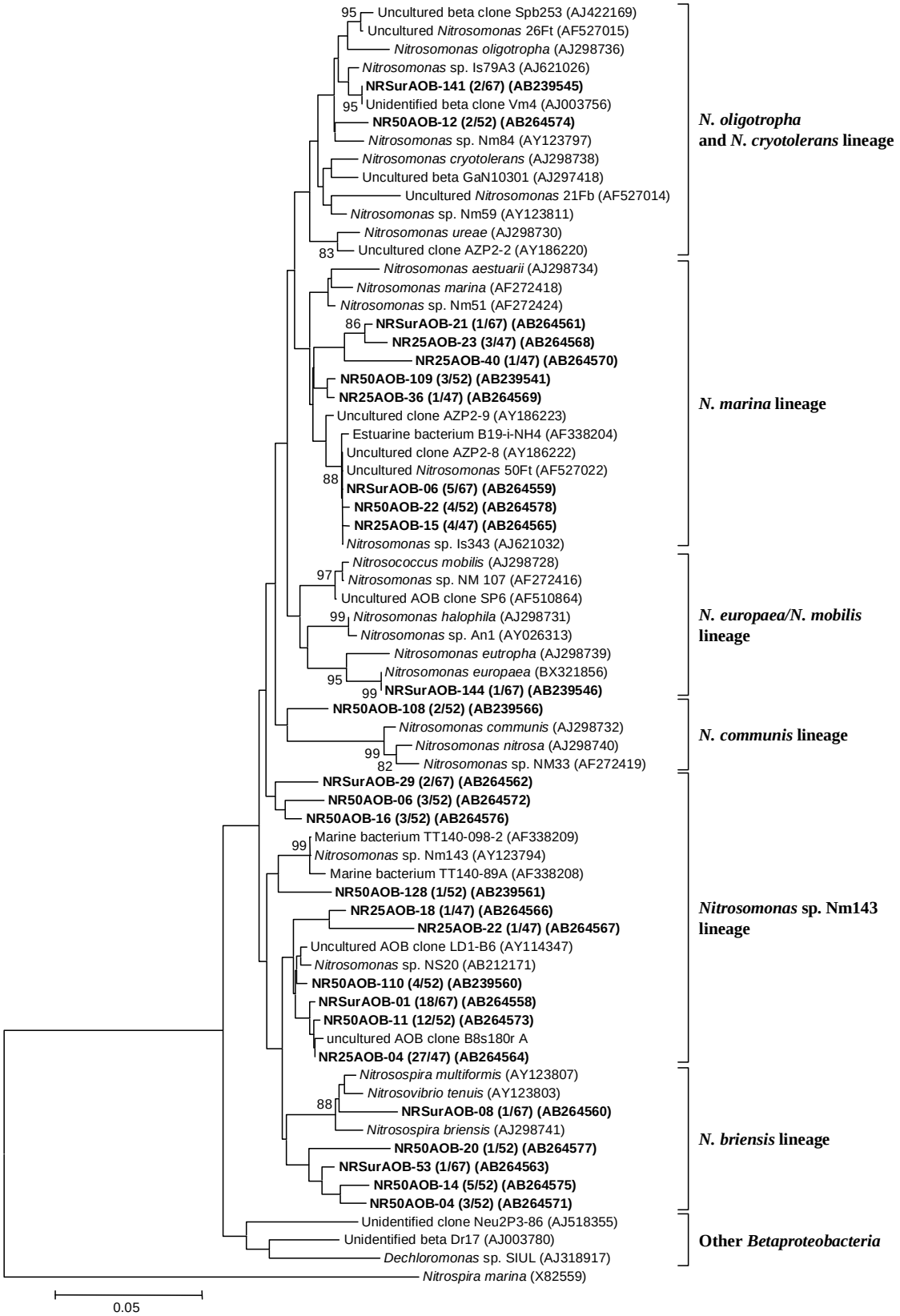

Fig. S2. Phylogenetic tree for the betaproteobacterial AOB, showing the positions of the clones obtained from three different points in the sediment. The tree was generated by

using 465 bp of the 16S rRNA genes and the neighbor-joining method. Scale bar = 5% sequence divergence. Parsimony bootstrap values of 70 or greater are presented at the nodes (from 100 replicates). The *N. marina* sequence (X82559) served as the outgroup for rooting the tree. The numbers in parentheses indicate the frequencies of appearance of identical clones in the total clones analyzed.

In contrast to the AOB community structure, information about community structure and abundance of NOB in intertidal sediments is scarce. Although *Nitrobacter* is the most commonly isolated and studied NOB from water environments, recent studies demonstrated the presence of *Nitrospira* as dominate NOB in sediments (1, 7, 12, 26). In this study, the *Nitrospira*-like NOB specific 16S rRNA gene copy numbers were one to three orders of magnitude higher than those of the *Nitrobacter*-like NOB (**Table 2**). Hence, the community structures of *Nitrospira*-like NOB in the sediment were further analyzed. Three 16S rRNA gene clone libraries of *Nitrospira*-like NOB were constructed from the SS, BW-25 and BW-50 samples (**Fig. 2** and **Table S1** in the supplemental material). Partial sequences of 510 bp were analyzed from 46, 44, and 46 clones randomly selected from the SS, BW-25 and BW-50 clone libraries, respectively. The diversity of the *Nitrospira*-like NOB clone libraries was very low and more than 97% of the clones analyzed were related to the *Nitrospira marina* lineage with 96-99% sequence similarity. Other clones were related to the *Nitrospira defluvii* lineage with 97-99% sequence similarity (**Table S1**). Thus, the *Nitrospira*-like NOB community structures in the burrow walls were also similar to that in the sediment surface. Similarly, presence of *Nitrospira marina*-like NOB in estuarine sediment was indicated by stable isotope probing analysis (12). *Nitrospira marina*-like

NOB were also detected in a submerged filter treating a high salinity industrial wastewater containing NH_4^+ and phenol (8) and in biofilms developed in freshwater or seawater aquaria (15).

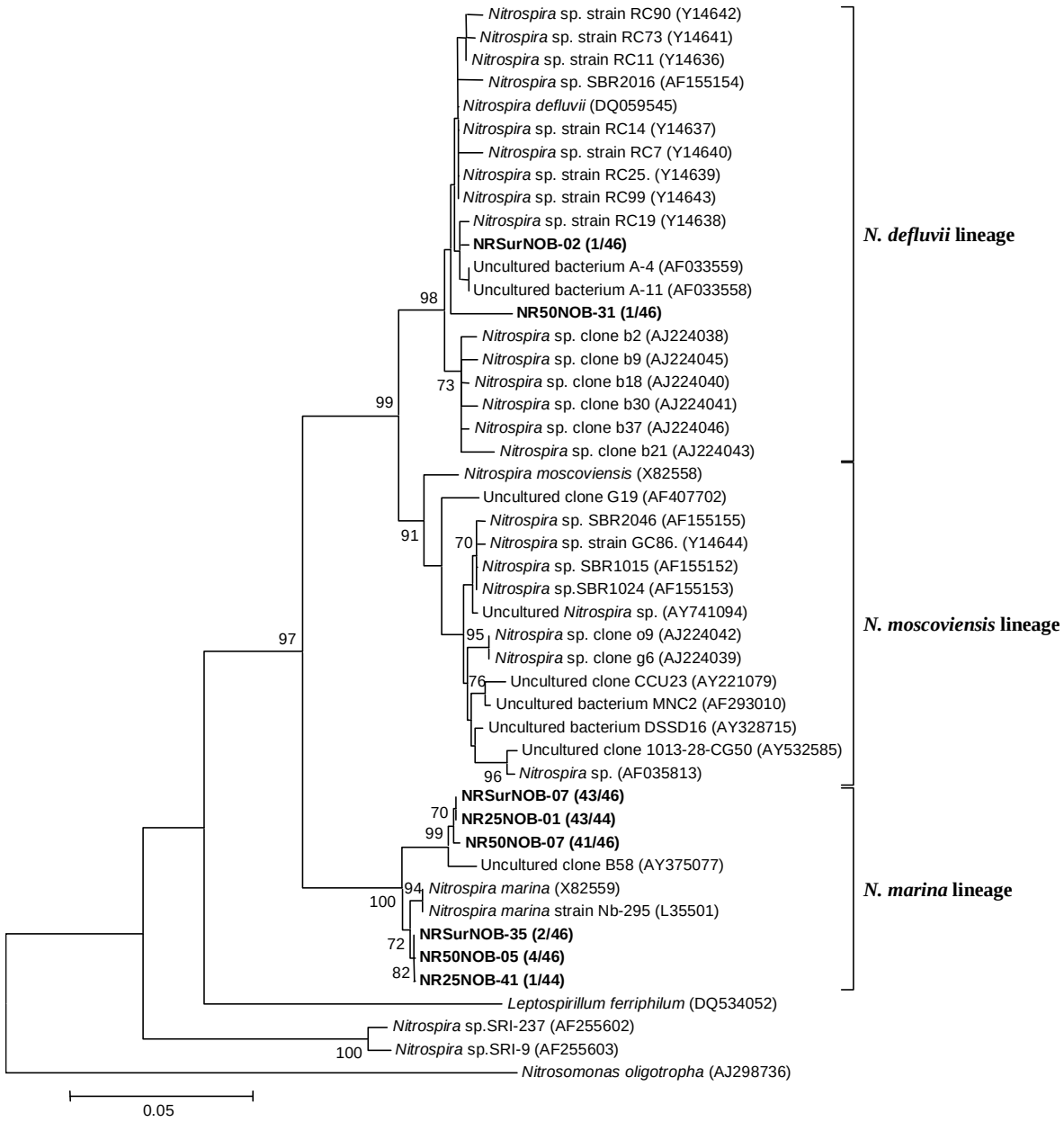

Fig. 2. Phylogenetic tree for *Nitrospira*-like NOB, showing the positions of the clones obtained from three different points in the sediment. The tree was generated by using 510 bp of the 16S rRNA genes and the neighbor-joining method. Scale bar = 5% sequence

divergence. Parsimony bootstrap values of 70 or greater are presented at the nodes (from 100 replicates). The *N. oligotropha* sequence (AJ298736) served as the outgroup for rooting the tree. The numbers in parentheses indicate the frequencies of appearance of identical clones in the total clones analyzed.

Microbial density

Total microbial cell counts were performed on different layers of the bulk sediment and the burrow wall samples (**Table 2**). The lateral average of total bacterial cell numbers was highest (6.5×10^9 cells cm^{-3}) at the sediment surface and slightly decreased with depth down to 4.0×10^9 cells cm^{-3} at a depth of 50-55 mm of the sediment. The cell numbers in the burrow wall were lower (1.0 to 1.9×10^9 cells cm^{-3}) than those of the bulk sediment samples ($P < 0.0001$, n=15) probably because the burrow walls were composed of loosely packed sediment (biofilms).

Betaproteobacterial AOB and *Nitrospira*- and *Nitrobacter*-like NOB specific 16S rRNA gene copy numbers were quantified by Q-PCR assay (**Table 2**). The AOB and *Nitrospira*-like NOB specific 16S rRNA gene copy numbers were in the range of 10^7 copies cm^{-3} except those at a depth of 50-55 mm of the bulk sediment. Presence of aerobic AOB in anoxic parts of the sediment could be explained by direct transport of AOB from the sediment surface by mixing, persistence of AOB, and capability of anoxic respiration of AOB. In contrast, the *Nitrobacter*-like NOB specific 16S rRNA gene copy numbers were one to three orders of magnitude lower than the *Nitrospira*-like NOB specific 16S rRNA gene copy numbers. Thus, *Nitrospira*-like NOB might be numerically dominant NOB in the intertidal sediment. The AOB and *Nitrospira*-like NOB specific 16S rRNA gene copy

numbers in the burrow walls (1.2 to 4.2 × 10^7 and 1.0 to 3.3 × 10^7 gene copies cm^{-3} for AOB and *Nitrospira*-like NOB, respectively) were comparable with those at the sediment surface (2.4 and 2.8 × 10^7 gene copies cm^{-3} for AOB and *Nitrospira*-like NOB, respectively) ($P > 0.05$, n = 4). These copy numbers slightly increased with depth in the burrow wall, whereas in the bulk sediment these copy numbers decreased with depth. Therefore, the AOB and *Nitrospira*-like NOB specific 16S rRNA gene copy numbers became higher in the burrow wall than in the bulk sediment at a depth of 50-55 mm ($P < 0.01$, n = 4).

Microelectrode measurements

The concentration profiles of O_2 and NH_4^+ were measured at a cross-section of the sediment (**Fig. 3A**). The microelectrodes were inserted into 4 points on the cross-section; the burrow wall at depths of 5 mm (point 1), 25 mm (point 2) and 50 mm (point 3), and the bulk sediment at a depth of 50 mm (point 4), as indicated in **Fig. 3B**. O_2 penetration depths were in the range of 0.6 to 1.2 mm at the cross-section of the sediment (**Fig. 3C**). The total O_2 consumption rates at the points 1, 2, 3 (i.e., in the burrow wall) and 4 (i.e., in the bulk sediment) were calculated to be 0.19, 0.21, 0.26 and 0.23 μmol cm^{-2} h^{-1}, respectively. Moreover, the O_2 concentrations at the sediment surface and bulk sediments at 5 mm and 25 mm were measured (data not shown) and the total O_2 consumption rates were calculated to be 0.20, 0.23 and 0.21 μmol cm^{-2} h^{-1}, respectively. NH_4^+ was consumed in the upper parts of the sediment at the points 1, 2 and 3, indicating high NH_4^+ consumption activity at the burrow wall (**Fig. 3D**). The total NH_4^+ consumption rates at the points 1, 2 and 3 were calculated to be 0.050, 0.026 and 0.033 μmol cm^{-2} h^{-1}, respectively. The total NH_4^+ consumption rates at the sediment surface and at the bulk sediment at a depth of 50 mm were

0.028 and 0.003 μmol cm^{-2} h^{-1}, respectively. Although O_2 consumption rates in the burrow wall were similar to those in the sediment surface ($P > 0.05$), the total NH_4^+ consumption rate at the point 1 was higher than that at the sediment surface ($P < 0.05$) and the rates at the points 2 and 3 were comparable to that at the sediment surface. NH_4^+ was produced in the deeper part of sediments at the points 3 and 4.

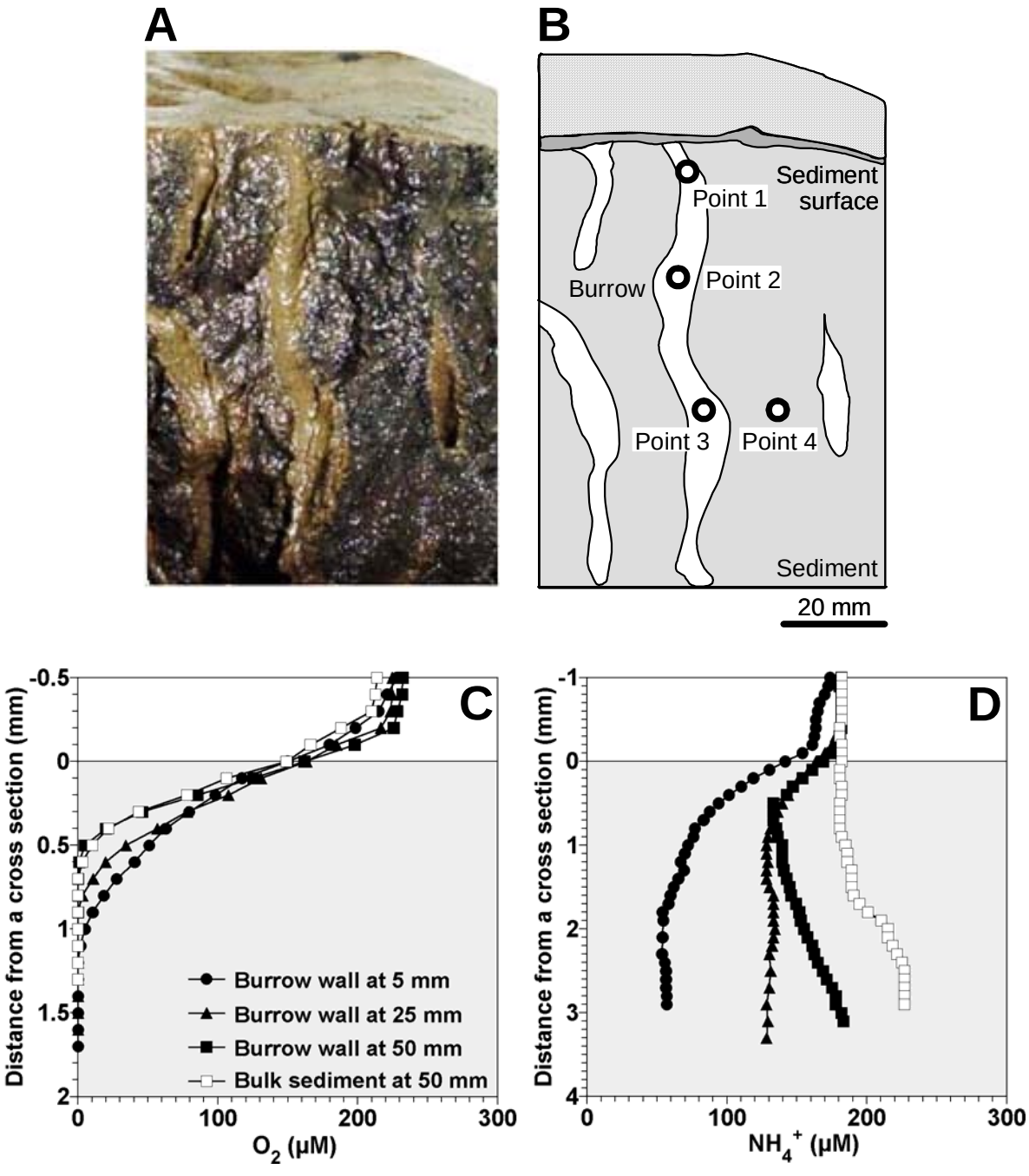

Fig. 3. Concentration profiles of O_2 and NH_4^+ at a cross-section of the sediment. (A) Photograph of the cross-section of the sediment. (B) A drawing of the cross-section of the sediment indicated in panel A. The points 1 to 4 in panel B indicate the points where the microelectrodes were inserted. (C and D) Concentration profiles of O_2 and NH_4^+ measured at each point, respectively. The profiles are average values (n = 3) and the standard deviations were less than 10% of the average values. Zero on the horizontal axis corresponds to the surface of the cross-section. The legends of panel D were the same as those in panel C.

Microelectrode measurements as well as Q-PCR assay demonstrated that the 16S rRNA gene copy numbers of AOB and *Nitrospira*-like NOB and the NH_4^+ consumption rates in the burrow walls were comparable with or higher than those in the sediment surface and in the bulk sediment (especially at a depth of 50-55 mm). These results indicate that infaunal burrows supported higher abundance of nitrifying bacteria and *in situ* NH_4^+ consumption activity in the burrow wall. These results were also consistent with the result of the microcosm experiments showing that increasing benthic infaunal density in the sediment resulted in the increases in NH_4^+ and total inorganic nitrogen consumption rates (**Fig. 1**). Mayer et al. showed that nitrification potentials in tube or burrow walls of 6 types of benthic macrofaunas were significantly greater than those of the surrounding bulk sediments (23). Furthermore, Dollhopf et al. found that coupled nitrification-denitrification was enhanced by macrofaunal burrowing activity in salt marsh sediments (11).

Many studies have aimed to measure solute concentrations in burrows (5, 13, 24, 25, 32, 34). However, all of the data were limited in the upper parts (a few cm depth) of the

sediments. In this study, we constructed and used the aquarium with agar slits in a sideboard to overcome this limitation (see **Fig. S1** in the supplemental material). The O_2 microelectrode was inserted into the center of the burrow at different depths through the agar slits and an O_2 concentration profile along the burrow structure was determined (**Fig. 4A**). A typical horizontal O_2 concentration profile was depicted in **Fig. 4B**. The O_2 concentration in the burrow decreased from 190 μM in the overlying water to 120 μM at a depth of 80 mm, but below which the decrease in the O_2 concentration was moderate (**Fig. 4A**). Thus, approximately 70 μM of O_2 still existed even at a depth of 350 mm. In contrast, O_2 penetration depth was only less than 1 mm below the sediment surface without infaunal burrows (data not shown). This was probably attributed to the infaunal irrigation activity to exchange the water with low concentrations of O_2 and nutrients with fresh water (19).

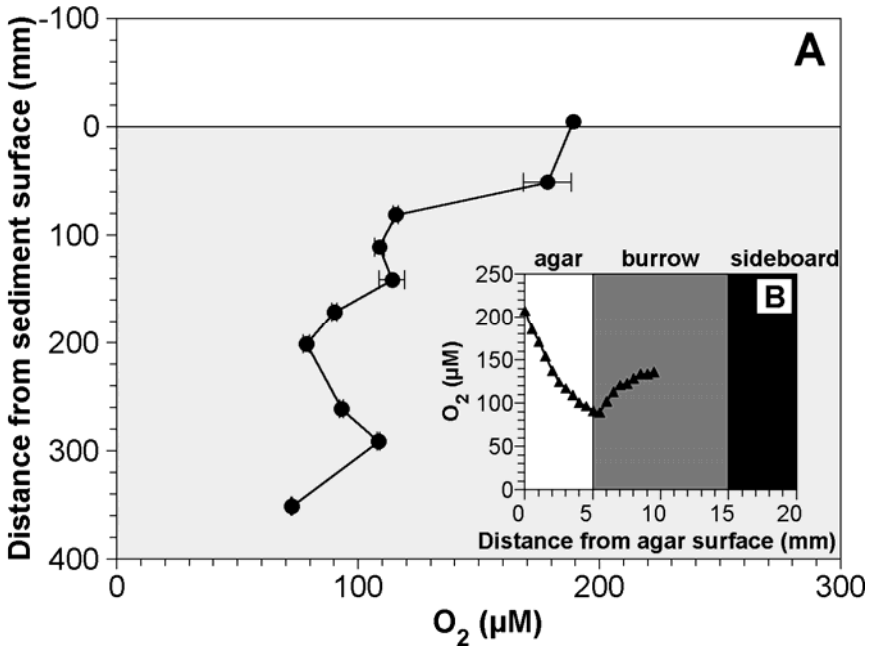

Fig. 4. A vertical O_2 concentration profile along an infaunal burrow measured in the aquarium with slits filled with agar plates in a sideboard (A). Data points were obtained

from the horizontal O_2 concentration profiles, as depicted in panel B, at different depths. The values indicate the average O_2 concentrations at the center of the burrow (i.e., 10 mm from agar surface in panel B). The error bars indicate the standard deviations of the measurements for 10 min at each position. A typical horizontal O_2 concentration profile in an infaunal burrow (B). An O_2 microelectrode was inserted into the center of a burrow through agar plate. Zero, 5 mm and 10 mm on the horizontal axis correspond to the agar surface, the agar-burrow interface and the center of the burrow, respectively.

The advantages of this method were to be able to know the exact position of burrows in sediment and to directly measure the concentration profiles in the burrows at the deeper parts of the sediment. However, O_2 diffused into the burrow and sediment through the agar plate, as indicated by the O_2 concentration gradients in the agar plate (**Fig. 4B**). The O_2 transport rates through the agar plate were, therefore, calculated from the O_2 concentration gradients in the agar plate based on Fick's first law of diffusion. The diffusion coefficient for O_2 in the 3% agar used for the calculation was 2.2×10^{-5} cm^2 s^{-1} (16). The mean O_2 transport rate was calculated to be 0.012 ± 0.001 μmol cm^{-2} h^{-1}. This value corresponded to ca. 5% of the total O_2 consumption rates in the burrow walls (0.19 to 0.26 μmol cm^{-2} h^{-1}). Thus, O_2 concentrations in the burrow would be slightly overestimated in this study. However, this does not negate the general trend in the results presented here.

In summary, combination of the 16S rRNA gene-based molecular approach and microelectrode measurements clearly demonstrated that the infaunal burrow facilitated O_2 transport into the sediment, which supported the higher abundance and *in situ* activity of nitrifying bacteria in the burrow walls in the intertidal sediment. Further studies with more

quantitative techniques such as fluorescent *in situ* hybridization (FISH) and microelectrodes for N_2O, NO_2^- and NO_3^- are desired to fully understand nitrogen cycling in the bioturbated sediment.

Acknowledgement

This work was partially supported by grant-in-aid (13650593) for developmental scientific research from the Ministry of Education, Science and Culture of Japan. Y. N. was supported by a research fellowship from the Japan Society for the Promotion of Science.

References

1. **Altmann, D., P. Stief, R. Amann, and D. de Beer.** 2004. Nitrification in freshwater sediments as influenced by insect larvae: quantification by microsensors and fluorescence in situ hybridization. Microb. Ecol. **48:**145-153.
2. **Altschul, S. F., W. Gish, W. Miller, E. W. Myers, and D. J. Lipman.** 1990. Basic local alignment search tool. J. Mol. Biol. **215:**403–410.
3. **Andrussow, L.** 1969. Diffusion, p. 513–727. *In* H. Borchers, H. Hauser, K. H. Hellwege, K. Schafer, and E. Schmidt (ed.), Landolt-Bornstein Zahlenwerte und Functionen, 6th ed., vol. II/5a. Springer, Berlin, Germany.
4. **Bernhard, A. E., T. Donn, A. E. Giblin, and D. A. Stahl.** 2005. Loss of diversity of ammonia-oxidizing bacteria correlates with increasing salinity in an estuary system. Environ. Microbiol. **7:**1289–1297.
5. **Binnerup, S. J., K. Jensen, N. P. Revsbech, M. H. Jensen, and J. Sørensen.** 1992. Denitrification, dissimilatory reduction of nitrate to ammonium, and nitrification in a

bioturbated estuarine sediment as measured with ^{15}N and microsensor techniques. Appl. Environ. Microbiol. **58:**303–313.

6. **Clesceri, L., A. Greenberg, and A. Eaton (ed.).** 1998**.** Standard methods for the examination of water and wastewater. American Public Health Association, Washington, D.C.

7. **Coci, M., D. Riechmann, P. L. E. Bodelier, S. Stefani, G. Zwart, and H. J. Laanbroek.** 2005. Effect of salinity on temporal and spatial dynamics of ammonia-oxidising bacteria from intertidal freshwater sediment. FEMS Microbiol. Ecol. **53:**359–368.

8. **Cortés-Lorenzo, C., M. L. Molina-Muñoz, B. Gómez-Villalba, R. Vilchez, A. Ramos, B. Rodelas, E. Hontoria, and J. González-López.** 2006. Analysis of community composition of biofilms in a submerged filter system for the removal of ammonia and phenol from industrial wastewater. Biochem. Soc. Trans. **34:**165–168.

9. **de Beer, D., A. Schramm, C. M. Santegoeds, and M. Kühl.** 1997. A nitrite microsensor for profiling environmental biofilms. Appl. Environ. Microbiol. **63:**973–977.

10. **Degrange, V., and R. Bardin.** 1995. Detection and counting of *Nitrobacter* populations in soil by PCR. Appl. Environ. Microbiol. **61:**2093–2098.

11. **Dollhopf, S. L., J. H. Hyun, A. C. Smith, H. J. Adams, S. O'Brien, and J. E. Kostka.** 2005. Quantification of ammonia-oxidizing bacteria and factors controlling nitrification in salt marsh sediments. Appl. Environ. Microbiol. **71:**240–246.

12. **Freitag, T. E., L. Chang, and J. I. Prosser.** 2006. Changes in the community structure and activity of betaproteobacterial ammonia-oxidizing sediment bacteria along a

freshwater–marine gradient. Environ. Microbiol. **8:**684–696.

13. **Glud, R. N., J. K. Gundersen, H. Røy, and B. B. Jørgensen.** 2003. Seasonal dynamics of benthic O_2 uptake in a semienclosed bay: Importance of diffusion and faunal activity. Limnol. Oceanogr. **48:**1265–1276.

14. **Hermansson, A., and P. E. Lindgren.** 2001. Quantification of ammonia-oxidizing bacteria in arable soil by real-time PCR. Appl. Environ. Microbiol. **67:**972–976.

15. **Hovanec, T. A., L. T. Taylor, A. Blakis, and E. F. Delong.** 1998. *Nitrospira*-like bacteria associated with nitrite oxidation in freshwater aquaria. Appl. Environ. Microbiol. **64:**258–264.

16. **Hulst, A. C., H. J. H. Hens, R. M. Buitelaar, and J. Tramper.** 1989. Determination of the effective diffusion coefficient of oxygen in gel materials in relation to gel concentration. Biotechnol. Tech. **3:**199–204.

17. **Koike, I., and H. Mukai.** 1983. Oxygen and inorganic nitrogen contents and fluxes in burrows of the shrimps *Callianassa japonica* and *Upogebia major*. Mar. Ecol. Prog. Ser. **12:**185–190.

18. **Kowalchuk, G. A., J. R. Stephen, W. De Boer, J. I. Prosser, T. M. Embley, and J. W. Woldendorp.** 1997. Analysis of ammonia-oxidizing bacteria of the β subdivision of the class Proteobacteria in coastal sand dunes by denaturing gradient gel electrophoresis and sequencing of PCR-amplified 16S ribosomal DNA fragments. Appl. Environ. Microbiol. **63**:1489-1497.

19. **Kristensen, E.** 1983. Ventilation and oxygen uptake by three species of *Nereis* (Annelida: Polychaeta). I. Effects of hypoxia. Mar. Ecol. Prog. Ser. **12:**289–297.

20. **López-García, P., F. Gaill, and D. Moreira.** 2002. Wide bacterial diversity associated

with tubes of the vent worm *Riftia pachyptila*. Environ. Microbiol. **4:**204–215.

21. **Maidak, B. L., G. L. Olsen, N. Larsen, R. Overbeek, M. J. McCaughey, and C. R. Woese.** 1997. The RDP (Ribosomal Database Project). Nucleic Acids Res. **25:**109–110.
22. **Matsui, G Y., D. B. Ringelberg, and C. R. Lovell.** 2004. Sulfate-reducing bacteria in tubes constructed by the marine infaunal polychaete *Diopatra cuprea*. Appl. Environ. Microbiol. **70:**7053–7065.
23. **Mayer, M. S., L. Schaffner, and W. M. Kemp.** 1995. Nitrification potentials of benthic macrofaunal tubes and burrow walls: effects of sediment NH_4^+ and animal irrigation behavior. Mar. Ecol. Prog. Ser. **121:**157–169.
24. **Meyers, M. B., H. Fossing, and E. N. Powell.** 1987. Microdistribution of interstitial meiofauna, oxygen and sulfide gradients, and the tubes of macro-infauna. Mar. Ecol. Prog. Ser. **35:**223–241.
25. **Meyers, M. B., E. N. Powell, and H. Fossing.** 1988. Movement of oxybiotic and thiobiotic meiofauna in response to changes in pore-water oxygen and sulfide gradients around macro-infaunal tubes. Mar. Biol. **98:**395–414.
26. **Nakamura, Y., H. Satoh, T. Kindaichi, and S. Okabe.** Community structure, abundance, and in situ activity of nitrifying bacteria in river sediments as determined by the combined use of molecular techniques and microelectrodes. Environ. Sci. Tech. **40:**1532–1539.
27. **Nakamura, Y., H. Satoh, S. Okabe, and Y. Watanabe.** 2004. Photosynthesis in sediments determined at high spatial resolution by the use of microelectrodes. Wat. Res. **38:**2440–2448.

28. **Okabe, S. H. Satoh, and Y. Watanabe.** 1999. In situ analysis of nitrifying biofilms as determined by in situ hybridization and the use of microelectrodes. Appl. Environ. Microbiol. **65:**3182–3191.

29. **Purkhold, U., M. Wagner, G. Timmermann, A. Pommerening-Röser, and H.-P. Koops.** 2003. 16S rRNA and *amo*A-based phylogeny of 12 novel betaproteobacterial ammonia-oxidizing isolates: extension of the dataset and proposal of a new lineage within the nitrosomonads. Int. J. Syst. Evol. Microbiol. **53:**1485-1494.

30. **Revsbech, N. P.** 1989. An oxygen microelectrode with a guard cathode. Limnol. Oceanogr. **34:**474–478.

31. **Steward, C. C., S. C. Nold, D. B. Ringelberg, D. C. White, and C. R. Lovell.** 1996. Microbial biomass and community structures in the burrows of bromophenol producing and non-producing marine worms and surrounding sediments. Mar. Ecol. Prog. Ser. **133:**149–165.

32. **Stief, P., D. Altmann, D. de Beer, R. Bieg, and A. Kureck.** 2004. Microbial activities in the burrow environment of the potamal mayfly *Ephoron virgo*. Freshw. Biol. **49:**1152–1163.

33. **Thompson, J. D., D. G. Higgins, and T. J. Gibson.** 1994. CLUSTAL W: improving the sensitivity of progressive multiple sequence alignment through sequence weighting, position-specific gap penalties and weight matrix choice. Nucleic Acids Res. **22:**4673–4680.

34. **Wang, F., A. Tessier, and L. Hare.** 2001. Oxygen measurements in the burrows of freshwater insects. Freshw. Biol. **46:**317–327.

TABLE 1. Detection frequency and phylogenetic relatives of the AOB clones analyzed at sediment surface (SS) and burrow walls (BW) at 25-30 mm and 50-55 mm from the sediment surface.

Lineage	No. of OTUs (No. of clones) in the following layer			
Closest relative	SS	BW-25	BW-50	Similarity
Total	8 (67)	7 (47)	12 (52)	
Nitrosomonas oligotropha lineage				
Nitrosomonas sp. Is79A3 (AJ621026)			1 (2)	95-98
Unidentified *Betaproteobacterium* Vm4 (AJ003756)	1 (2)			99
Nitrosomonas marina lineage				
Nitrosomonas sp. Is343 (AJ621032)	1 (5)	1 (4)	1 (4)	97-99
Uncultured bacterium clone AZP2-9 (AY186223)	1 (1)	3 (5)	1 (3)	95-98
Nitrosomonas europaea/*Nitrosococcus mobilis* lineage				
Nitrosomonas europaea (BX321856)	1 (1)			99
Nitrosomonas communis lineage				
Nitrosomonas communis (AJ298732)			1 (2)	95
Nitrosomonas sp. Nm143 lineage				
Uncultured AOB clone B8s180r (AB212150)	1 (18)	1 (27)	1 (12)	95-99
Nitrosomonas sp. Nm143 (AY123794)	1 (2)		3 (7)	94-96
Nitrosomonas sp. NS20 (AB212171)		2 (2)	1 (4)	93-98
Nitrosospira briensis lineage				
Nitrosospira multiformis (AY123807)	2 (2)		3(9)	94-97

TABLE 2. Summary of total microbial cell counts and 16S rRNA gene copy numbers of AOB and *Nitrospira*- and *Nitrobacter*-like NOB in the bulk sediment and burrow wall samples.

Sediment depth	Total cell (10^9 cells cm^{-3})[a]		AOB (10^7 copies cm^{-3})[a]		*Nitrospira* (10^7 copies cm^{-3})[a]		*Nitrobacter* (10^7 copies cm^{-3})[a]	
	Sediment	Burrow	Sediment	Burrow	Sediment	Burrow	Sediment	Burrow
0-5 mm (surface)	6.5 ± 0.7	N.D.[b]	2.4 ± 0.3	N.D.[b]	2.8 ± 1.8	N.D.[b]	0.1 ± 0.0	N.D.[b]
5-10 mm	5.4 ± 1.3	1.3 ± 0.3	2.8 ± 1.4	1.2 ± 0.8	5.7 ± 4.1	1.0 ± 0.9	0.1 ± 0.1	0.3 ± 0.0
25-30 mm	4.7 ± 1.0	1.0 ± 0.1	3.0 ± 0.9	3.0 ± 0.5	1.1 ± 0.8	1.4 ± 0.1	0.2 ± 0.1	0.3 ± 0.1
50-55 mm	4.0 ± 0.5	1.9 ± 0.7	0.7 ± 0.2	4.2 ± 1.7	0.6 ± 0.2	3.3 ± 0.2	0.004 ± 0.003	0.2 ± 0.1

[a] The values are averages ± standard deviations.

[b] N.D. : not determined.

TABLE S1. Detection frequency and phylogenetic relatives of the *Nitrospira*-like NOB clones analyzed at sediment surface (SS) and burrow walls (BW) at 25-30 mm and 50-55 mm from the sediment surface.

Lineage	No. of OTUs (No. of clones)			
Closest relative	SS	BW-25	BW-50	Similarity
Total	3 (46)	2 (44)	3 (46)	
Nitrospira marina lineage				
Uncultured bacterium clone B58 (AY375077)	1 (43)	1 (43)	1 (41)	96-99
Nitrospira marina (X82559)	1 (2)	1 (1)	1 (4)	98-99
Nitrospira defluvii lineage				
Nitrospira defluvii (DQ059545)	1 (1)			99
Nitrospira sp. clone b2 (AJ224038)			1 (1)	97